THE JOURNAL OF BIOLOGICAL CHEMISTRY VOL. 286, NO. 23, pp. 20208–20216, June 10, 2011

Cell Cycle-dependent Phosphorylation and Ubiquitination of a G Protein α Subunit*[S]

Received for publication, March 11, 2011, and in revised form, April 24, 2011 Published, JBC Papers in Press, April 26, 2011, DOI 10.1074/jbc.M111.239343

Matthew P. Torres, Sarah T. Clement, Steven D. Cappell, and Henrik G. Dohlman[1]

From the Department of Biochemistry and Biophysics, University of North Carolina at Chapel Hill, Chapel Hill. NC 27599-7260

A diverse array of external stimuli, including most hormones and neurotransmitters, bind to cell surface receptors that activate G proteins. Mating pheromones in yeast *Saccharomyces cerevisiae* activate G protein-coupled receptors and initiate events leading to cell cycle arrest in G_1 phase. Here, we show that the Gα subunit (Gpa1) is phosphorylated and ubiquitinated in response to changes in the cell cycle. We systematically screened 109 gene deletion strains representing the non-essential yeast kinome and identified a single kinase gene, *ELM1*, as necessary and sufficient for Gpa1 phosphorylation. Elm1 is expressed in a cell cycle-dependent manner, primarily at S and G_2/M. Accordingly, phosphorylation of Gpa1 in G_2/M phase leads to polyubiquitination in G_1 phase. These findings demonstrate that Gpa1 is dynamically regulated. More broadly, they reveal how G proteins can simultaneously regulate, and become regulated by, progression through the cell cycle.

G protein coupled receptors and heterotrimeric G proteins are the predominant components through which cells receive and transduce extracellular signals. G protein signal transduction is highly conserved throughout eukaryotes, including the yeast *Saccharomyces cerevisiae*. In yeast, haploid **a**-type cells secrete an **a**-factor pheromone that binds to receptors on the surface of α-type cells, whereas α-type cells secrete an α-factor that acts exclusively on **a**-type cells (1). Consequently, the haploid cells fuse to form an **a**/α diploid cell.

As with other G protein systems, activation of the yeast pheromone receptor stimulates exchange of GDP for GTP on the G protein α subunit (Gpa1),[2] which promotes its dissociation from the Gβγ (Ste4/18) heterodimer (1, 2). In yeast, Gβγ is primarily responsible for transmission and amplification of the signal to effector proteins, whereas the Gα subunit serves primarily to regulate the levels of free Gβγ. As a consequence, cells are highly sensitive to small changes in the stoichiometry of Gα and Gβγ (3–5). The signal is terminated by hydrolysis of GTP to GDP on the Gα subunit, which promotes reassociation of the heterotrimeric G protein complex. Further regulation is imposed by accelerating the GTPase activity of Gα via regulators of G protein signaling proteins (6).

Propagation of the G protein signal requires components of a MAPK cascade (Ste20, Ste11, Ste7, Fus3, or Kss1), a MAPK scaffold (Ste5), as well as a transcription factor (Ste12) (1). Consequently, the pheromone initiates changes in gene expression and cell morphology that prepare the cell to undergo cell-cell and nuclear fusion. Critical to this process is the initiation of cell cycle arrest in G_1 phase, which ensures that each haploid cell contains exactly one copy of every chromosome before fusion (7). Pheromone-induced G_1 arrest necessarily prevents fusion during DNA replication (S phase) or before mitosis (M phase), during which nuclear fusion could lead to missegregation of genetic material, aneuploidy, and other proliferative disadvantages (8, 9). Consequently, yeast mating and cell cycle progression must be highly coordinated processes.

The mating pathway is well known to regulate the cell cycle by stimulating expression of Far1, a cyclin-dependent kinase inhibitor that arrests cells at START in late G_1 phase (10–14). Reciprocally, Far1 is itself regulated in a cell cycle-dependent manner and is degraded after cells pass through START and exit G_1 phase (10, 11). Degradation of Far1 is initiated in G_1 by cyclin-dependent kinase-mediated phosphorylation, which promotes its ubiquitination by the SCF (Skp1/Cullin/F-box) ubiquitin ligase (13, 15, 16).

Emerging evidence suggests that multiple mating pathway components are regulated by ubiquitination. Targets of ubiquitin-mediated degradation include the regulator of G protein signaling protein Sst2 (17), the MAPK kinase Ste7 (18), the MAPK scaffold protein Ste5 (19), and the G protein α subunit Gpa1 (20–23). Of these, the SCF has been shown to be necessary and sufficient for ubiquitination of Gpa1 (4). While SCF substrates are generally phosphorylated prior to ubiquitination (24, 25), as yet the kinase that phosphorylates Gpa1 has not been identified.

Here we identify a novel G protein kinase, Elm1. We show that the G protein is phosphorylated directly by Elm1 and that phosphorylation occurs in coordination with Elm1 expression during the cell cycle. G protein phosphorylation in G_2/M phase leads to ubiquitination during the following G_1 phase. In the absence of Elm1, the G protein is neither phosphorylated nor ubiquitinated. Taken together, these findings show how G proteins can simultaneously regulate, and become regulated by, progression through the cell cycle.

EXPERIMENTAL PROCEDURES

Strains and Plasmids—Standard methods for growth, maintenance, and transformation of yeast and bacteria were used

* This work was supported, in whole or in part, by National Institutes of Health Grants R01 GM059167 and R01 GM080739 (to H. G. D.) and R01 GM080739-S1 and K99 GM094533-01 (to M. P. T.).

[S] The on-line version of this article (available at http://www.jbc.org) contains supplemental Tables 1 and 2, Figs. 1–5, and additional references.

To whom correspondence should be addressed: Dept. of Biochemistry and Biophysics, University of North Carolina at Chapel Hill, Genetic Medicine Bldg., 120 Mason Farm Rd., Suite 3010, Chapel Hill, NC 27599-7260; Tel.: 919-843-6894; E-mail: hdohlman@med.unc.edu.

[2] The abbreviations used are: Gpa1, G protein α subunit; SCF, Skp1/Cullin/F-box; PIPES, 1,4-piperazinediethanesulfonic acid; UD, ubiquitination domain.

throughout. To ensure accurate cell density comparisons, a diluted fraction of each cell culture was lightly sonicated before measurement at an $A_{600\ nm}$ to break apart cell clusters that commonly form between *elm1*Δ cells. Strains used in this study were BY4741 (*MAT***a** *leu2*Δ *met15*Δ *his3*Δ *ura3*Δ), *elm1*Δ (BY4741 *elm1*Δ::KanMX4), *ELM1-TAP* (Yeast TAP-fusion library, Open Biosystems), *cdc6-1* (BY4741 *cdc6-1 hph*) (provided by Jean Cook, University of North Carolina), 15Dau (*MAT***a** *ade1 his2 leu2–3, trp1–112, ura3*Δ), *cdc28-1* (15Dau, *cdc28-1*) (provided by Beverly Errede, University of North Carolina), LHY488 (*MAT***a** *his3-*Δ*200 leu2*Δ*1 ura3–52 lys2–801 trp1*Δ*63 ade2–101*), LHY489 (LHY488 *cim3-1*) (provided by Linda Hicke, Northwestern University) (26), MTY235 (*MAT***a** *ade2-1 his3–11,15 leu2–3,112 trp1-1 ura3-1 can1–100*), MTY670 (MTY235 *cdc34-2*), and MTY668 (MTY235 *cdc4-1*) (provided by Mike Tyers, Samuel Lunenfield Research Institute) (27). Integrated yeast strains were constructed by plasmid integration of pRS406-GPA1-(81-1539 bp) or pRS406-GPA1-(81-1539 bp)^{S200A} at the naturally occurring HindIII site within *GPA1*, resulting in a single full-length copy of *GPA1* at its endogenous locus. Integration was validated by immunoblotting with wild-type cells to confirm loss of the phosphorylation dependent mobility shift (in the case of S200A). All experiments were done in BY4741 unless otherwise specified. Table of yeast strains used in this study are shown in supplemental Table 1.

Plasmid Construction—Yeast shuttle plasmids pRS315-ELM1 and pRS316-ELM1 were constructed by PCR amplification of *ELM1* ± 500 bp flanking the open reading frame (primers SalI-ELM1-F and SacI-ELM1-R) and directional cloning into the SalI and SacI sites of pRS315 or pRS316. Single point mutations (Gpa1^{S200A}, Gpa1^{S200E}, and Elm1^{K117R}) were constructed by QuikChange (Stratagene) mutagenesis using the indicated primers (supplemental Table 2). Plasmids containing *gpa1*$^{15S/T-A}$ were constructed by chemical synthesis of a 413-bp fragment of *GPA1* (base pairs 392–786 of the open reading frame starting from the naturally occurring HindIII restriction site of *GPA1*) within which all serine and threonine codons were mutated to alanine, and a silent BglII site was introduced by mutation of base pairs 781 and 783 (GenScript). The synthesized fragment was cloned into *GPA1* plasmids in which the same silent BglII mutation was introduced by QuikChange (using primer GPA1-BglII-F/R), followed by restriction digestion with HindIII and BglII. pYEX 4T-1-GST-ELM1 was purified from the yeast GST-fusion library host strain EJ 758 (28) using a yeast plasmid miniprep kit (Zymo Research) and then retransformed into BY4741 *elm1*Δ cells for expression of GST-Elm1. All plasmids were verified by DNA sequencing.

Growth Arrest and Release—Log-phase cell cultures were arrested in G_1 phase with a synthetic α-factor peptide (30 μM final concentration, CHI Scientific 53424), in S phase by addition of hydroxyurea (added in powder form to 10 mg/ml final concentration, Sigma Aldrich H8627), and in G_2/M phase by addition of nocodazole (15 μg/ml final concentration, Sigma Aldrich M1404). Note that for G_2/M phase arrest, cells were first treated with 1% dimethyl sulfoxide for 30 min at 30 °C, followed by addition of nocodazole (100× stock at 1.5 mg/ml in dimethyl sulfoxide), resulting in a 2% final concentration of dimethyl sulfoxide in the cell culture. Each arrest was allowed to proceed for 2.5 h at 30 °C unless otherwise noted. Cells were released from arrest by centrifugation and washing with 3 × 100 ml of sterile water followed by resuspension in fresh medium to an $A_{600\ nm}$ of 0.7 and growth at 30 °C.

Growth of Temperature-sensitive Mutants—Temperature-sensitive mutants (*cdc6-1, cdc28-1, cdc4-1,* or *cdc34-2*) and the isogenic wild type counterstrains were grown at a permissive temperature (25 °C) to early log-phase and then shifted to the restrictive temperature (37 °C) for 2.5 h to induce cell cycle arrest in G_1 phase (*cdc28-1* cells), or early S phase (*cdc6-1* cells) and for 1 h to inactivate the SCF ubiquitin ligase (*cdc4-1* or *cdc34-2* cells).

In Vivo Ubiquitination Assays—Gpa1 polyubiquitination was detected by constitutive (*ADH1* promoter) expression of Gpa1 in yeast harboring a temperature-sensitive proteasome mutation (*cim3-1*) or by coexpression of Gpa1 and Myc-ubiquitin as described previously (22). For *cim3-1* and isogenic wild type cells, log-phase cultures were grown at the permissive temperature (25 °C) to an $A_{600\ nm}$ of 0.5–0.6, followed by transition to the restrictive temperature (37 °C) for 3 h. Inducible Myc-ubiquitin strains were grown at 30 °C to an $A_{600\ nm}$ of 0.5–0.6, followed by addition of $CuSO_4$ to 100 μM for 3 h at 30 °C as described previously (29). Detection of Gpa1 ubiquitination at different cell cycle stages was accomplished by arresting log-phase cells followed by induction of Myc-ubiquitin expression for 3 h.

Protein Detection—Unless otherwise noted, cell pellets were harvested by addition of 100% trichloroacetic acid (5% final concentration), centrifugation at 4000 × *g* for 1 min, washing with 1 ml of 10 mM NaN_3, and then stored as a frozen cell pellet at −80 °C. Protein extracts were generated by glass bead lysis in trichloroacetic acid as described previously (30) and resolved by 10% SDS-PAGE and immunoblotting. Membranes were probed with anti-Gpa1 at 1:1000 (31), anti-FLAG at 1:1000 (F1804, Sigma Aldrich), anti-Clb2 at 1:350 (sc-9071, Santa Cruz Biotechnology), anti-p44/42 at 1:500 (9101L, Cell Signaling Technology), anti-Kss1 at 1:350 (sc-6775, Santa Cruz Biotechnology), anti-Fus3 at 1:350 (sc-6773, Santa Cruz Biotechnology), anti-G6PDH at 1:50,000 (A9521, Sigma Aldrich), anti-Myc at 1:100 (9E10 mouse monoclonal antibody), and anti-protein A at 1:50,000 (P3775, Sigma Aldrich). Immunoreactive species were visualized by chemiluminescent detection (PerkinElmer Life Sciences) of horseradish peroxidase-conjugated anti-rabbit (170-5046) or anti-mouse IgG (170-5047) (Bio-Rad). Where indicated, image densitometry was conducted using National Institutes of Health ImageJ software (32). Statistical analysis was conducted using GraphPad Prism 4 for a minimum of three independent experiments unless noted otherwise.

Phosphatase Assays—Cells grown to an $A_{600\ nm}$ of 1.0 were harvested by centrifugation at 2000 × *g* and stored at −80 °C. Cell pellets were resuspended in 1× λ phosphatase buffer (New England Biolabs) containing 50 mM HEPES (pH 7.5), 100 mM NaCl, 2 mM DTT, 0.01% Brij 35, 1 mM $MnCl_2$, and 1× EDTA-free protease inhibitors (Roche). Each resuspended pellet was split in half and subjected to glass bead lysis in the presence or absence of phosphatase inhibitors (50 mM NaF and 1.3 mM sodium orthovanadate) (S6508, Sigma Aldrich). Lysates were

centrifuged at 21,000 × *g* for 15 min, and the supernatant fraction was then collected into a fresh tube with or without 60 units (2.25 units/μl final concentration) of λ protein phosphatase (New England Biolabs) for 30 min at 30 °C. The reaction was stopped by addition of 6× SDS-PAGE loading buffer, and the samples were immediately subjected to SDS-PAGE and immunoblot analysis. Alternatively, phosphatase assays were conducted on purified protein. Briefly, 1 μl of yeast-purified Gpa1-FLAG was diluted in 1× λ-phosphatase buffer with or without 20 units (2 units/μl final concentration) λ protein phosphatase.

GST-Elm1 Expression, Purification, and in Vitro Kinase Assay—1 liter cultures of *elm1*Δ cells harboring pYEX-4T1-GST-ELM1 or elm1^{K117R} were grown to an $A_{600\ nm}$ of 0.7 and treated with 500 μM $CuSO_4$ for 2 h to induce expression of GST-Elm1. Cells were harvested, washed with water, and stored at −80 °C. The cell pellets were subjected to glass bead lysis in buffer containing 20 mM Tris-HCl (pH 8.0), 400 mM NaCl, 2 mM $MgCl_2$, 5% glycerol, 0.1% Triton X-100 (Sigma Aldrich), 1 mM DTT, 1× protease inhibitor mixture tablets, and 500 μM PMSF. The lysate mixture was subjected to microcentrifugation at 21,000 × *g* for 10 min, and GST-Elm1 was purified from the soluble extract using glutathione-Sepharose™ 4 Fast-flow (GE Healthcare) followed by washing with buffer containing 20 mM Tris-HCl (pH 8.0), 400 mM NaCl, 2 mM $MgCl_2$, 5% glycerol, and 1 mM DTT and elution with dialysis buffer containing 20 mM glutathione (pH 7.5). Eluted protein was dialyzed with a slide-a-lyzer mini cartridge (Pierce) into kinase storage buffer containing 20 mM Tris-HCl (pH 8.0), 100 mM NaCl, 2 mM $MgCl_2$, and 5% glycerol. *In vitro* kinase assays were conducted by incubating 0.08–0.16 pmol of purified GST-Elm1 (3.2–6.4 nM final concentration) and 12.5–25 pmol of recombinant purified Gpa1 or indicated mutants (0.5–1 μM final concentration) in 1× kinase reaction buffer previously described for *in vitro* Elm1 kinase assays and containing 50 mM Tris-HCl (pH 7.5), 10 mM $MgCl_2$, 5 mM DTT, 2 mM EGTA, 200 mM sodium orthovanadate, and 10 μCi of [γ-^{32}P]ATP (PerkinElmer Life Sciences) for 1 h at 30 °C (33). Reactions were stopped by addition of 6× SDS-PAGE loading buffer and immediately subjected to SDS-PAGE. The resulting gel was dehydrated and exposed to autoradiography film (HyBlot CL, Denville Scientific).

Affinity Purification of Gpa1-FLAG—Yeast harboring pRS316-ADH-GPA1-FLAG was grown to early log-phase and then harvested by centrifugation. The resulting cell pellet was lysed, and Gpa1-FLAG was purified as described previously (4).

Gene Transcription Assay—Pheromone-dependent transcription reporter assays were conducted as described previously (34). Briefly, cell cultures at an $A_{600\ nm}$ of 0.8 were dispensed (90 μl into each of 48 wells of a 96-well plate) and mixed with 10 μl of α-factor peptide at the indicated concentration for 90 min at 30 °C. Next, each well was mixed with 20 μl of FDG solution (130 mM PIPES (pH 7.2), 0.25% Triton-X100, 0.5 mM fluorescein di-β-galactopyranoside (Marker Gene Technologies, M0250)) for 1 h at 37 °C. The reaction was stopped by the addition of 20 μl of 1 M sodium bicarbonate followed by fluorescence quantification using a fluorescence plate reader (SpectraMax M5, Molecular Devices).

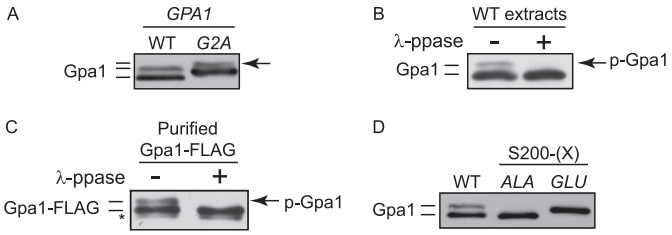

FIGURE 1. **Phosphorylation induces an electrophoretic mobility shift in Gpa1.** Immunoblot analysis of Gpa1 using Gpa1-specific antibodies. *A*, cells over-expressing wild-type *GPA1* (pAD4M-GPA1) (*WT*) or the myristoylation-site mutant *GPA1*^{G2A} (*G2A*) analyzed by immunoblotting. The *arrow* marks the position of the presumptive phosphorylated form of Gpa1. *B*, soluble protein extracts from cells overexpressing wild-type Gpa1 were split into two separate aliquots, and one half was treated (+) with λ-protein phosphatase. *p-Gpa1*, phosphorylated Gpa1. *C*, Gpa1-FLAG purified from nocodazole-arrested cells and treated (+) with λ-protein phosphatase (*ppase*). *D*, wild type cells overexpressing wild-type Gpa1 (*WT*) or phosphorylation site mutants (S200A, *ALA* or S200E, *GLU*). *, nonspecific immunoblot band.

Escherichia coli Expression of His$_6$ Fusion Proteins—Recombinant His$_6$-Gpa1 was expressed by autoinduction as described previously (35). All procedures were conducted at 4 °C unless noted otherwise. Briefly, competent BL21-RIPL cells (Stratagene) were transformed with the indicated expression vector. 5 ml of saturated starter cultures (containing ZY medium (10 g/l tryptone, 5 g/l yeast extract) with 15 mg of glucose, 50 μg/ml carbenicillin, 25 μg/ml chloramphenicol) were used to inoculate 800 ml of ZY medium containing 1× *M* solution (25 mM Na_2HPO_4, 25 mM KH_2PO_4, 50 mM NH_4Cl, 5 mM Na_2SO_4), 1× *5052* solution (0.5% (w/v) glycerol, 0.5% (w/v) glucose, 10% (w/v) α-lactose), 50 mM $MgSO_4$, 50 μg/ml carbenicillin, and 25 μg/ml chloramphenicol. Cultures were grown for 8 h at 37 °C and then shifted to 18 °C overnight. The G protein was purified by nickel-affinity chromatography as described previously (23) but without cleavage of the N-terminal His$_6$ tag. The resultant protein was dialyzed by slide-a-lyzer (Pierce) in 20 mM Tris (pH 8.0), 100 mM NaCl, 2 mM $MgCl_2$, 20 μM GDP, and 0.5 mM tris(2-carboxyethyl)phosphine.

RESULTS

Gpa1 Is a Phosphoprotein—Gpa1 undergoes a variety of post-translational modifications, including myristoylation, palmitoylation, and ubiquitination (21, 36). The myristoylation state of Gpa1 can be distinguished by an electrophoretic mobility shift following SDS-PAGE and immunoblotting. Because only a fraction of Gpa1 is mobility-shifted under these conditions, the prevailing view has been that Gpa1 exists in both myristoylated and non-myristoylated states (37). However, upon close inspection of overexpressed protein, we found that even non-myristoylated Gpa1^{G2A} exhibits differential mobility by immunoblotting, indicating the presence of another modification (Fig. 1*A*). Given that phosphorylation can likewise alter the electrophoretic mobility of proteins, we asked whether phosphorylation rather than myristoylation might account for the second form of Gpa1. Consistent with this hypothesis, phosphatase treatment of whole cell extracts (Fig. 1*B*) or of purified Gpa1 (*C*) resulted in complete loss of the slower migrating form of Gpa1. We also found that mutation of serine 200, which was identified as a phosphorylation site by mass spectrometry (38), altered the mobility of Gpa1. Substitution of Ser-200 with alanine (S200A)

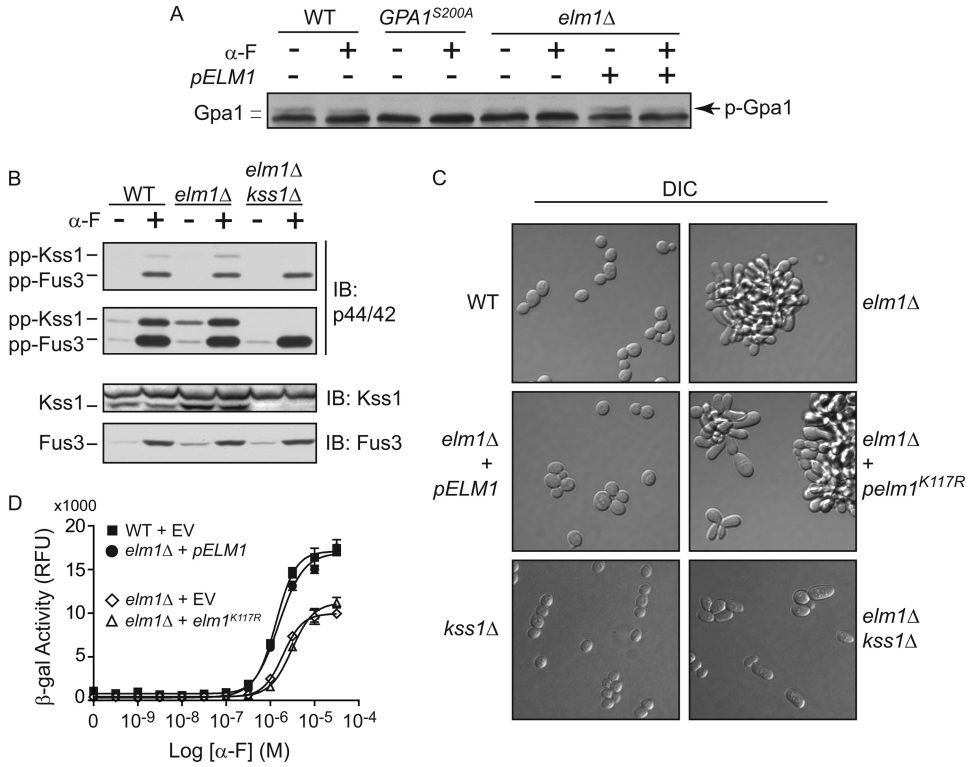

FIGURE 2. **Yeast kinome screen reveals Elm1 as a Gpa1 kinase.** The abundance of phosphorylated Gpa1 was determined by immunoblotting 109 different kinase gene deletion strains. A single kinase, Elm1, is required for detection of phosphorylated Gpa1. *A*, validation of kinome screen results. Wild-type cells (*WT*) or cells expressing *GPA1*^{S200A} (by gene replacement) or *elm1*Δ cells harboring empty vector or plasmid-borne *ELM1* (*ELM1*). *B*, analysis of pheromone-dependent (+) MAP kinase activation (*top panels*, different exposures) and total expression (*bottom panels*) in WT, *elm1*Δ, and *elm1*Δ *kss1*Δ cells. *IB*, immunoblot. *C*, differential interference contrast (*DIC*) images of yeast strains used in the pheromone signaling assays shown in *B* and *D*. *D*, analysis of pheromone-dependent gene transcription in *elm1*Δ cells with the indicated plasmid containing *ELM1*, *elm1*^{K117R}, or an empty vector (*EV*). Indicated are yeast strains expressing a *FUS1-lacZ* reporter treated with the indicated concentrations of mating pheromone. Results show the mean ± S.E. for four individual experiments, each performed in quadruplicate. *RFU*, relative fluorescence units.

or glutamate (S200E) replicated the mobility of dephosphorylated and phosphorylated Gpa1, respectively (Fig. 1*D*). We conclude that Gpa1 is a phosphorylated protein.

A Yeast Kinome Screen Reveals Elm1 as a G Protein Kinase—To identify the Gpa1 kinase, we monitored the phosphorylation-dependent mobility shift of endogenously expressed Gpa1 in gene deletion strains representing the majority of the yeast kinome. Of the 109 strains tested, deletion of *ELM1* alone resulted in a significant observable loss of phosphorylated Gpa1. Phosphorylation of Gpa1 was restored by plasmid-borne expression of *ELM1* (Fig. 2*A*). We observed no such differences in the absence of kinases that act downstream of Elm1 or that are functionally similar to Elm1 (see discussion, supplemental Fig. 1*A*) (33, 39). In addition to testing kinase deletions, we also monitored Gpa1 phosphorylation in each of 31 phosphatase-deletion strains, including all those involved in the pheromone response, but did not observe any difference in the abundance of phosphorylated Gpa1 (supplemental Fig. 1*C*). We conclude that Elm1 phosphorylates Gpa1 *in vivo*.

Elm1 Is Required for Maximal Pheromone-induced Gene Transcription—Elm1 is best known as a regulator of cell morphology during G_2/M phase of the cell cycle. During G_2/M, Elm1 phosphorylates proteins required for the morphogenesis checkpoint that coordinates bud emergence and mitosis (40, 41) as well as for organization of septins during cytokinesis (33, 39, 42). Yeast harboring *elm1* mutations exhibit a morphologically distinct growth pattern in which cells delay cytokinesis and undergo elongated bud growth, a process that also occurs under conditions of nitrogen starvation and filamentous growth (43). Elm1 has been proposed to inhibit the filamentous growth response that includes multiple signaling pathway branches, including (but not limited to) the MAP kinases Ste20, Ste11, Ste7, and Kss1 (43, 44), all of which participate as well in the pheromone response pathway. Accordingly, we found that Kss1 was more highly expressed and activated in *elm1*Δ compared with wild-type cells (Fig. 2*B*). In addition, deletion of *KSS1* in *elm1*Δ cells reduced the filamentous-like phenotype (elongated buds and flocculation) typical of *elm1*Δ cells (Fig. 2*C*). In contrast, the other pheromone-responsive MAP kinase, Fus3, was largely unaffected by the absence of Elm1 (Fig. 2*B*).

We next determined whether Elm1 regulates pheromone-dependent gene transcription using a β-galactosidase reporter fused with the promoter of the mating-specific gene *FUS1*. We found that *elm1*Δ cells exhibit a significantly reduced maximum level of pheromone-induced gene transcription. Signaling was restored upon plasmid-borne expression of wild-type Elm1 but not kinase-inactive Elm1^{K117R} (Fig. 2*D*). Thus, Elm1 represses activation of the MAP kinase branch of the filamentous growth response, including Kss1, and is required for maximum response to the pheromone.

Gpa1 Is Phosphorylated Directly by Elm1—Elm1 clearly plays a role in multiple signaling pathways, including the filamentous

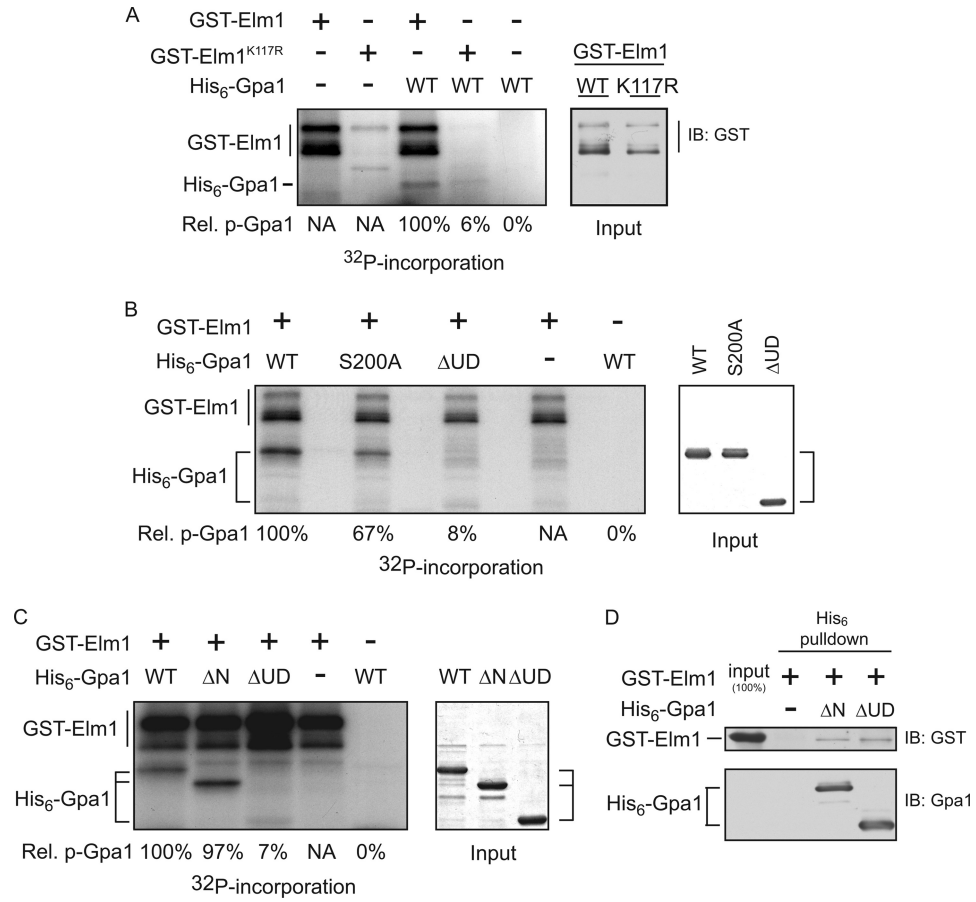

FIGURE 3. **Elm1 is necessary and sufficient for Gpa1 phosphorylation.** The association between Elm1 and Gpa1 as determined by copurification and by *in vitro* kinase assay. *A*, *in vitro* kinase assay with purified GST-Elm1 or catalytically inactive GST-Elm1^{K117R} and purified recombinant Gpa1 in the presence of [γ^{32}P]ATP (*left panel*) and GST-Elm1 input detected by immunoblot with anti-GST (*right panel*). *B*, *in vitro* kinase assay with GST-Elm1 and purified recombinant Gpa1 (*WT*), Gpa1^{S200A} (S200A), or Gpa1$^{\Delta 1\text{-}36,\Delta 129\text{-}236}$ (ΔUD) in the presence of [γ^{32}P]ATP. Shown is the incorporation of radioactive phosphate (*left panel*) and Gpa1 input detected by Coomassie staining (*right panel*). *C*, *in vitro* kinase assay with GST-Elm1 and with purified recombinant His$_6$-tagged Gpa1 (*WT*), Gpa1$^{\Delta 1\text{-}36}$ (Δ*N*), or Gpa1$^{\Delta 1\text{-}36,\ \Delta 129\text{-}236}$ (Δ*UD*) lacking the ubiquitinated subdomain. Shown is the incorporation of radioactive phosphate (*left panel*) and Gpa1 input detected by Coomassie gel staining (*right panel*). *D*, *in vitro* affinity purification using nickel affinity matrix and immunodetection of bound GST-Elm1 described in *C*. Relative ^{32}P incorporation (*Rel. p-Gpa1*) is shown for Gpa1 and was calculated as follows: [^{32}P signal/Coomassie signal]$_{mutant}$/[^{32}P signal/Coomassie signal]$_{WT}$.

growth and pheromone response pathways, any of which could be indirectly responsible for the diminished Gpa1 phosphorylation in *elm1*Δ cells. Therefore, we asked whether Elm1 acts directly on Gpa1. We established that purified Elm1 can bind to and phosphorylate recombinant Gpa1 *in vitro* (Fig. 3). Elm1 is capable of autophosphorylation (43), and we show that this activity is exhibited as well by GST-Elm1 (Fig. 3, *A*–*C*). Both Elm1 autophosphorylation and Gpa1 transphosphorylation were blocked when catalytically inactive GST-Elm1^{K117R} was substituted for the wild-type kinase (Fig. 3*A*). Consistent with our findings *in vivo*, Ser-200 is required for maximum phosphorylation of Gpa1 (Fig. 3*B*). Similar results were observed upon mutation of all 15 Ser and Thr residues in the ubiquitination domain (data not shown). Finally, Elm1 was able to bind to, but not effectively phosphorylate, Gpa1$^{\Delta UD}$, a mutant that lacks the ubiquitination domain of the protein (residues 129–236) (Fig. 3, *C* and *D*). We conclude that Elm1 phosphorylates Gpa1 directly at Ser-200 and multiple other sites throughout the protein.

Gpa1 Phosphorylation Is Cell Cycle-dependent—We next determined how phosphorylation of Gpa1 is regulated. Elm1 is expressed primarily during S and G_2/M phases of the cell cycle (42, 43, 45), a phenotype that we corroborated (supplemental Fig. 2). Further, longstanding evidence indicates that the mobility-shifted (phosphorylated) form of Gpa1 is significantly reduced upon pheromone stimulation (31), which induces cell cycle arrest in G_1 phase. Thus, we considered whether Gpa1 phosphorylation is regulated during the cell cycle. We directly compared Gpa1 from cells arrested in G_1 phase with α-factor (α-F), in S phase with hydroxyurea, or in G_2/M phase with nocodazole. Hydroxyurea inhibits deoxyribonucleotide synthesis, inducing a DNA replication checkpoint arrest in S phase (46). Nocodazole inhibits microtubule polymerization and induces a checkpoint arrest at the metaphase/anaphase transition of mitosis (47). We found that phosphorylated Gpa1 is most abundant in cells arrested in S and G_2/M phase but lowest in cells arrested in G_1 phase (Fig. 4*A*). To determine the dynamics of phosphorylation during the cell cycle, we monitored Gpa1 during arrest and release in cells treated with nocodazole or hydroxyurea. To validate the arrest and release protocol, we monitored changes in the mitotic cyclin Clb2 (48). We found that phosphorylated Gpa1 accumulates in a coordinated fashion with Clb2 as cells arrest in either G_2/M or S phase (Fig. 4, *B* and *D*). Upon release from nocodazole, phosphorylated Gpa1

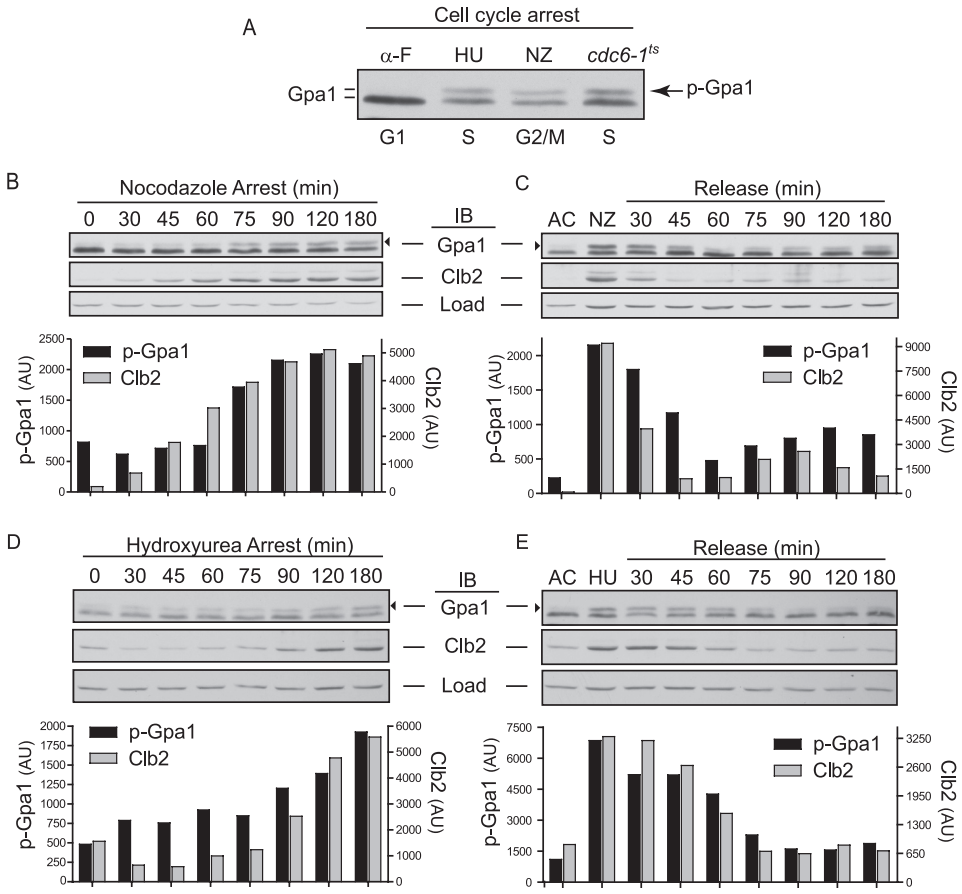

FIGURE 4. **Gpa1 phosphorylation is cell cycle-dependent.** Cells treated for 2.5 h with α-factor pheromone (*α-F*, arrests cells in G_1 phase), hydroxyurea (*HU*, arrests cells in S phase) or nocodazole (*NZ*, arrests cells in G_2/M phase) followed by release into fresh medium where indicated. Shown are aliquots taken at the indicated time points followed by immunoblotting. The abundance of phosphorylated Gpa1 (*black arrowhead*) and Clb2 were quantified by densitometry from the immunoblot shown above. *AU*, arbitrary units; *AC*, asynchronous cells; *Load*, G6PDH loading control. *A*, direct comparison of Gpa1 from arrested cells. Cells were also arrested in late G_1/early S phase by temperature shift of *cdc6-1* cells. *B*, nocodazole arrest. *C*, nocodazole release. *D*, hydroxyurea arrest. *E*, hydroxyurea release.

and Clb2 rapidly decrease in abundance and then increase concomitantly as cells reenter the cell cycle (Fig. 4*C* and supplemental Fig. 3). Similar coordination between phosphorylated Gpa1 and Clb2 was evident in cells released from hydroxyurea-induced cell cycle arrest (Fig. 4E). Finally, we observed temperature-dependent accumulation of phosphorylated Gpa1 in *cdc6–1*^{ts} cells, which are incapable of DNA replication licensing, resulting in a post-START arrest in late G_1/early S phase (Fig. 4*A*) (49, 50). We conclude that Gpa1 phosphorylation is Elm1-dependent and cell cycle-regulated. Although phosphorylated Gpa1 accumulates throughout the S and G_2/M phases, it is rapidly eliminated from cells during G_1 phase.

Elm1 Is Required for Gpa1 Polyubiquitination—We have shown previously that Gpa1 is polyubiquitinated by the SCF^{Cdc4} ubiquitin ligase (4) and that ubiquitination occurs primarily at lysine 165 within the ubiquitinated subdomain of Gpa1 (21). Typically, SCF recruits phosphorylated proteins as substrates for ubiquitination (24, 25). Therefore, we asked whether Elm1 phosphorylation promotes Gpa1 polyubiquitination. We compared Gpa1 polyubiquitination in the presence and absence of *ELM1* using a proteasome-deficient yeast strain, *cim3–1* (22, 23). For these experiments, Gpa1 was overexpressed to allow detection of the minor ubiquitinated species. Growth of *cim3–1* cells at the restrictive temperature inactivates Cim3, an essential protein component of the 26 S proteasome (51), thereby stabilizing polyubiquitinated proteins and further enabling their detection by immunoblotting. Consistent with the hypothesis, Gpa1 polyubiquitination is considerably diminished in the absence of Elm1 or in the presence of plasmid-borne $Elm1^{K117R}$ (Fig. 5). To validate the observations made in *cim3–1* cells, we also monitored Gpa1 polyubiquitination in wild-type or *elm1*Δ cells expressing myc-ubiquitin (proteins conjugated to myc-ubiquitin are degraded slowly) (supplemental Fig. 4) (52, 53). Once again Gpa1 polyubiquitination was diminished in the absence of Elm1. We conclude that Elm1 is required for ubiquitination, as well as for phosphorylation, of Gpa1.

Gpa1 Ubiquitination Is Regulated during the Cell Cycle—Phosphorylation is a well established precursor to ubiquitination by the SCF (25) and serves as a signal for recruitment of target substrates by F-box proteins (54). Our previous findings indicate that Gpa1 is ubiquitinated by SCF^{Cdc4}. The data presented above indicate that Gpa1 is phosphorylated by Elm1 and that Elm1 is required for ubiquitination. Therefore, we postulated that phosphorylation by Elm1 precedes ubiquitination by SCF. To test this hypothesis, we compared the relative proportion of phosphorylated Gpa1 in cells lacking functional Cdc4 (F-box protein) or Cdc34 (ubiquitin-conjugating enzyme),

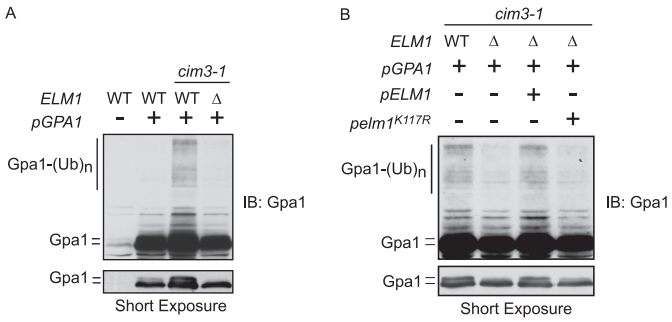

FIGURE 5. **Elm1 is required for Gpa1 polyubiquitination.** Temperature-sensitive proteasome-deficient (*cim3-1* or *cim3-1/elm1*Δ) or isogenic wild-type cells overexpressing the indicated form of plasmid-borne *GPA1* (pAD4M-GPA1, *GPA1*) grown at the restrictive temperature. *A*, accumulation of Gpa1 polyubiquitination in *cim3-1 versus cim3-1/elm1*Δ. *B*, accumulation of Gpa1 polyubiquitination in *cim3-1* or *cim3-1/elm1*Δ cells with or without plasmid expression of *ELM1* or *elm1*^{K117R}.

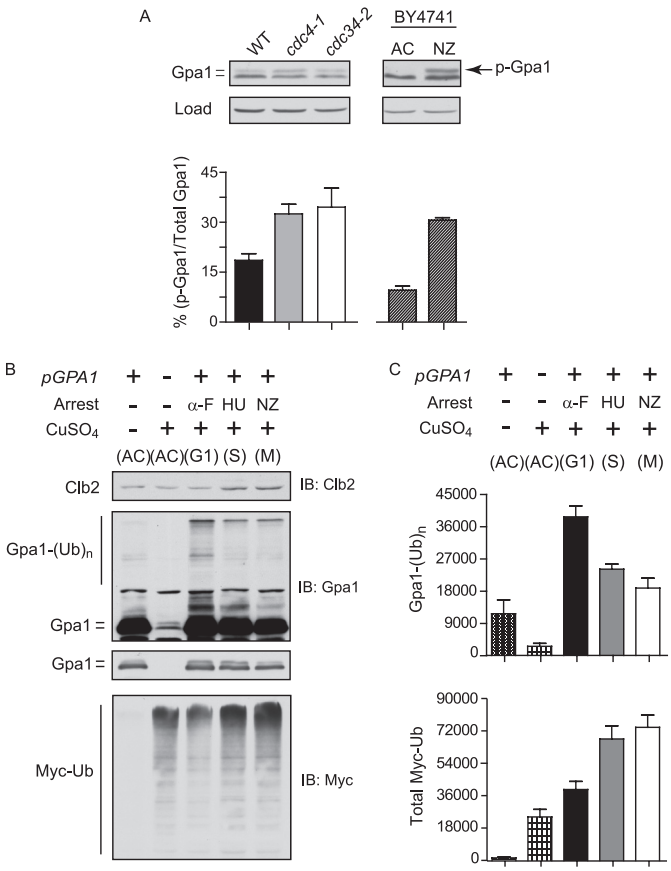

FIGURE 6. **Gpa1 polyubiquitination by SCF^{Cdc4} is cell cycle-regulated.** Gpa1 phosphorylation in SCF mutant strains or Gpa1 polyubiquitination under different cell cycle arrested conditions. *A*, accumulation of phosphorylated Gpa1 (*p-Gpa1*) in cells lacking functional SCF^{Cdc4}. Gpa1 immunoblot analysis of whole cell extracts from temperature-sensitive *cdc4-1* or *cdc34-2* mutant strains, or the isogenic wild-type strain. The *bar graph* represents the ratio of phosphorylated Gpa1 (*top band*) to the sum total of Gpa1 (*top* and *bottom bands*) expressed as a percentage (*left panel*). Shown is the same analysis conducted for Gpa1 from asynchronous (*AC*) or nocodazole-arrested (*NZ*) wild-type cells (*right panel*). Results are the mean ± S.E. for three independent experiments analyzed in triplicate. *B*, accumulation of Gpa1 polyubiquitination (from plasmid pAD4M, *top panel*) or total Myc-ubiquitin (*bottom panel*) in wild type BY4741 cells harboring copper-inducible myc-ubiquitin and arrested in G_1 phase with α-factor (*α-F*), in S phase with hydroxyurea (*HU*), or in G_2/M phase with nocodazole (*NZ*), followed by $CuSO_4$ induction of Myc-ubiquitin. *C*, quantitation of absolute immunoblot intensity for ubiquitinated Gpa1 and Myc-ubiquitin (*Myc-Ub*) from *B*. Results are the mean ± S.E. for three independent experiments analyzed in triplicate.

which we previously identified as responsible for polyubiquitination of Gpa1 (4). Accordingly, we monitored Gpa1 in temperature-sensitive *cdc4-1* and *cdc34-2* mutants (27). Consistent with the hypothesis, we found the proportion of phosphorylated Gpa1 to be higher in asynchronous cells lacking active forms of either Cdc4 or Cdc34 but comparatively lower in identically treated wild-type cells (Fig. 6*A*, *left panel*). Similar results were obtained using Tet-repressible versions of *CDC4* and *CDC34* (data not shown). Thus, phosphorylated Gpa1 accumulates in the absence of functional SCF^{Cdc4} ubiquitin ligase.

Finally, we considered whether ubiquitination, in addition to phosphorylation, might be regulated by the cell cycle. In support of this model, accumulation of phosphorylated Gpa1 in SCF-deficient cells is comparable with that observed in G_2/M-arrested cells (Fig. 6*A*, *right panel*). Moreover, we found that Gpa1 polyubiquitination is significantly higher in cells arrested in G_1 phase with α-factor mating pheromone or by temperature inactivation of *cdc28-1* when compared with cells arrested in S phase or in G_2/M phase (Fig. 6, *B* and *C*, and supplemental Fig. 5). Although treatment with α-factor results in Far1-mediated G_1 arrest, cells expressing *cdc28-1* undergo G_1 arrest independent of pheromone pathway activation at the restrictive temperature (55). In either case, Gpa1 polyubiquitination is highest in cells arrested in G_1 phase. Taken together, the data presented here reveal that Gpa1 is dynamically regulated. Phosphorylation and ubiquitination are independent of the pheromone stimulus and therefore not the result of feedback regulation. Rather, these modifications occur in conjunction with the cell cycle. Thus, the G protein is simultaneously a regulator of, and regulated by, cell cycle progression.

DISCUSSION

It is now well established that the G protein α subunit Gpa1 is ubiquitinated. Here we have begun to discern how this ubiquitination event is regulated. Our investigation began by showing that Gpa1 is phosphorylated and that phosphorylation results in an electrophoretic mobility shift of the protein. This property allowed us to determine that a single kinase (Elm1) is necessary for proper phosphorylation *in vivo*. Using purified components, we showed that Elm1 is also sufficient for Gpa1 phosphorylation *in vitro*. Elm1 is expressed primarily in S and G_2/M phases of the cell cycle. Correspondingly, we found that the G protein is phosphorylated in a cell cycle-dependent manner. Gpa1 is polyubiquitinated by SCF, and phosphorylation is typically required for SCF-mediated ubiquitination. Thus, we investigated whether phosphorylation leads to ubiquitination of Gpa1 and whether ubiquitination also occurs in a cell cycle-dependent manner. Indeed, although Gpa1 phosphorylation peaks in G_2/M phase, ubiquitination occurs in the subsequent G_1 phase. These findings establish that G proteins can be regulated by progression through the cell cycle. More broadly, they raise the possibility that other pathway components may also be subject to cell cycle regulation.

The participation of Elm1 in G protein signaling was unexpected. Elm1 is best known as a protein kinase that coordinates events leading to cell division, including bud emergence, mitosis, and cytokinesis (33, 39–43). In this capacity, Elm1 phos-

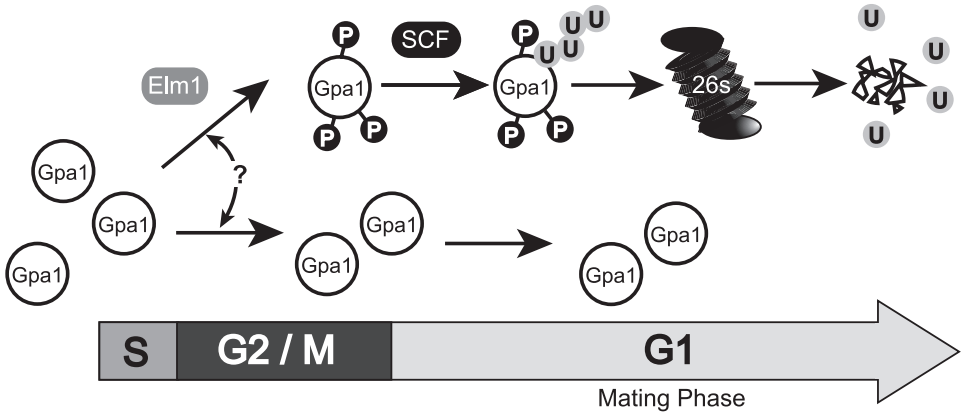

FIGURE 7. **Model of cell cycle G protein regulation.** Elm1 phosphorylates a subpopulation of Gpa1 during S and G_2/M phase. Phosphorylated Gpa1 is stable until entrance into the following G_1 phase, when it is targeted for polyubiquitination by the SCF^{Cdc4} ubiquitin ligase. The selective mechanism responsible for initiating phosphorylation of a fraction of the total G protein population is unknown (*?*) but may be due to cellular localization of signal transduction complexes near the bud neck of a dividing cell where Elm1 is localized during the S and G_2/M phases. Localization-specific cell cycle-dependent ubiquitination of Gpa1 may provide a mechanism to optimize the local stoichiometry of Gα relative to Gβγ subunits and restrict signaling competency to G_1 phase of the cell cycle.

phorylates protein kinases involved in septin organization and cytokinesis (Gin4 and Cla4) (33, 39, 42), another kinase that phosphorylates and deactivates the morphogenesis checkpoint protein Swe1 (Hsl1) (40, 41), and a fourth kinase that inhibits the mitotic exit network when the spindle position checkpoint is activated (Kin4) (56). It is unlikely that Gpa1 is regulated by any of these Elm1 substrates, given that deletion of those genes has no effect on Gpa1 phosphorylation or pheromone responsiveness. Thus, Gpa1 represents a new target of Elm1.

Whereas *elm1*Δ was the only mutant that exhibited a loss of Gpa1 phosphorylation, some residual phosphorylation could still be detected *in vivo* (Fig. 2*A*). Therefore, we speculate that Gpa1 is phosphorylated by another kinase. Possibilities include kinases that are absent from the gene deletion array, kinases essential for cell viability, and kinases that have functions related to Elm1. Elm1 is one of three closely related kinases, including Tos3 and Sak1. All three proteins are known to phosphorylate and activate Snf1 (the yeast homolog of human AMPK (5′ AMP-activated protein kinase), primarily under conditions of glucose starvation (57). Under the normal growth conditions used to assess mating pheromone responses however, deletion of *TOS3*, *SAK1*, or *SNF1* does not appear to affect Gpa1 phosphorylation or pheromone signaling (supplemental Fig. 1A). Taken together, our findings indicate that Elm1 is largely responsible for Gpa1 phosphorylation, is uniquely able to regulate the pheromone response pathway, and does so in a cell cycle-dependent manner.

Other lines of evidence support the model that Elm1 phosphorylates Gpa1. First, Gpa1 is neither phosphorylated nor ubiquitinated when Elm1 is absent. In contrast, we did not observe any such differences in the absence of 108 other kinases. Second, we did not observe any differences in the absence of 31 different protein phosphatases. Thus it is unlikely that Elm1 acts indirectly by inhibiting the function of a Gpa1-phosphatase. Third, we detected a substantial accumulation of phosphorylated Gpa1 in the absence of the SCF function. Finally, we detected a substantial enrichment of Gpa1 polyubiquitination in G_1-arrested cells as compared with S or G_2/M-arrested cell cultures. These data confirm that phosphorylation and ubiquitination occur in a cell cycle-dependent manner and that phosphorylation precedes ubiquitination.

As the primary negative regulator of the mating pathway, Gpa1 is a logical target for regulation by posttranslational modifications. We have shown that pheromone-dependent gene transcription is diminished in cells that lack Elm1 function. Similarly, pheromone-dependent gene transcription is diminished in cells expressing $Gpa1^{\Delta UD}$. $Gpa1^{\Delta UD}$ lacks a domain (UD, residues 129–236) that is required for ubiquitination by SCF as well as phosphorylation by Elm1 (4, 21, 22). The Gpa1 ubiquitination domain cannot be the only target of phosphorylation, however, because mutation of all 15 serine and threonine residues within this region failed to diminish phosphorylation *in vitro* (data not shown) or ubiquitination *in vivo* (supplemental Fig. 4). Thus, alternate phosphorylation sites are likely to exist, and these may likewise target the protein for polyubiquitination, at least under some circumstances. Taken together, these data indicate that phosphorylation can occur at multiple sites throughout the protein, whereas ubiquitination is restricted to a specific subdomain of the protein.

We have now identified the primary components necessary for Gpa1 phosphorylation (Elm1) and polyubiquitination (SCF). While much has been learned, substantive questions remain. For instance, we have yet to establish how Elm1 and SCF work together to modulate G protein function. All existing data indicate redundancy within this process because perturbations to phosphorylation or ubiquitination have modest effects on G protein stability. Selective pressure in yeast may have instilled this property because cells lacking Gpa1 cannot grow as a result of G_1 cell cycle arrest. Alternatively phosphorylation and ubiquitination may affect G protein signaling in other ways. For example, ubiquitination could affect G protein catalytic activity. Ubiquitination could also serve to restrict Gpa1 localization to specific signal transduction complexes. Considering that Elm1 is localized predominately to the bud neck between dividing cells, Gpa1 phosphorylation and subsequent polyubiquitination may occur only during cell division or within a specialized subdomain of the plasma membrane (Fig. 7). Indeed,

Gpa1 was recently shown to concentrate to the bud neck during G_2/M phase, where Elm1 is located (58).

The yeast mating response is perhaps the best-characterized of any signal transduction system, yet it continues to reveal new mechanisms of signal regulation. It has long been known that pheromone stimulation activates the G protein and promotes cell cycle arrest in G_1. We now find that the G protein α subunit is phosphorylated and ubiquitinated in a manner that is contingent on cell cycle progression. The abundance of phosphorylated Gpa1 increases as cells progress through the S and G_2/M phases and decreases rapidly after cells divide and enter G_1 phase. Taken together, these data show that the G protein can be dynamically regulated. More broadly, these findings reveal a previously unsuspected degree of coordination between G protein signaling and cell division.

Acknowledgments—We thank Daniel Isom for constructive discussions and technical assistance with analysis of G protein point mutants, Candice Carlile and Jean Cook for the cdc6-1 yeast strain, and Rachael Baker and Jeffrey Duffy for plasmids.

REFERENCES

1. Dohlman, H. G., and Thorner, J. W. (2001) *Annu. Rev. Biochem.* **70,** 703–754
2. Sprang, S. R. (1997) *Annu. Rev. Biochem.* **66,** 639–678
3. Cole, G. M., Stone, D. E., and Reed, S. I. (1990) *Mol. Cell. Biol.* **10,** 510–517
4. Cappell, S. D., Baker, R., Skowyra, D., and Dohlman, H. G. (2010) *Mol. Cell* **38,** 746–757
5. Spain, B. H., Koo, D., Ramakrishnan, M., Dzudzor, B., and Colicelli, J. (1995) *J. Biol. Chem.* **270,** 25435–25444
6. Hepler, J. R. (2003) *Mol. Pharmacol.* **64,** 547–549
7. Wittenberg, C., and La Valle, R. (2003) *BioEssays* **25,** 856–867
8. Torres, E. M., Sokolsky, T., Tucker, C. M., Chan, L. Y., Boselli, M., Dunham, M. J., and Amon, A. (2007) *Science* **317,** 916–924
9. Torres, E. M., Williams, B. R., and Amon, A. (2008) *Genetics* **179,** 737–746
10. McKinney, J. D., Chang, F., Heintz, N., and Cross, F. R. (1993) *Genes Dev.* **7,** 833–843
11. Peter, M., Gartner, A., Horecka, J., Ammerer, G., and Herskowitz, I. (1993) *Cell* **73,** 747–760
12. Tyers, M., and Futcher, B. (1993) *Mol. Cell. Biol.* **13,** 5659–5669
13. Oehlen, L. J., and Cross, F. R. (1994) *Genes Dev.* **8,** 1058–1070
14. Peter, M., and Herskowitz, I. (1994) *Science* **265,** 1228–1231
15. Blondel, M., Galan, J. M., Chi, Y., Lafourcade, C., Longaretti, C., Deshaies, R. J., and Peter, M. (2000) *EMBO J.* **19,** 6085–6097
16. Henchoz, S., Chi, Y., Catarin, B., Herskowitz, I., Deshaies, R. J., and Peter, M. (1997) *Genes Dev.* **11,** 3046–3060
17. Hao, N., Yildirim, N., Wang, Y., Elston, T. C., and Dohlman, H. G. (2003) *J. Biol. Chem.* **278,** 46506–46515
18. Wang, Y., Ge, Q., Houston, D., Thorner, J., Errede, B., and Dohlman, H. G. (2003) *J. Biol. Chem.* **278,** 22284–22289
19. Garrenton, L. S., Braunwarth, A., Irniger, S., Hurt, E., Künzler, M., and Thorner, J. (2009) *Mol. Cell. Biol.* **29,** 582–601
20. Madura, K., and Varshavsky, A. (1994) *Science* **265,** 1454–1458
21. Marotti, L. A., Jr., Newitt, R., Wang, Y., Aebersold, R., and Dohlman, H. G. (2002) *Biochemistry* **41,** 5067–5074
22. Wang, Y., Marotti, L. A., Jr., Lee, M. J., and Dohlman, H. G. (2005) *J. Biol. Chem.* **280,** 284–291
23. Torres, M. P., Lee, M. J., Ding, F., Purbeck, C., Kuhlman, B., Dokholyan, N. V., and Dohlman, H. G. (2009) *J. Biol. Chem.* **284,** 8940–8950
24. Deshaies, R. J. (1999) *Annu. Rev. Cell Dev. Biol.* **15,** 435–467
25. Willems, A. R., Goh, T., Taylor, L., Chernushevich, I., Shevchenko, A., and Tyers, M. (1999) *Philos Trans. R. Soc. Lond. B Biol. Sci.* **354,** 1533–1550
26. Ghislain, M., Udvardy, A., and Mann, C. (1993) *Nature* **366,** 358–362
27. Tang, X., Orlicky, S., Liu, Q., Willems, A., Sicheri, F., and Tyers, M. (2005) *Methods Enzymol.* **399,** 433–458
28. Martzen, M. R., McCraith, S. M., Spinelli, S. L., Torres, F. M., Fields, S., Grayhack, E. J., and Phizicky, E. M. (1999) *Science* **286,** 1153–1155
29. Roth, A. F., Sullivan, D. M., and Davis, N. G. (1998) *J. Cell Biol.* **142,** 949–961
30. Lee, M. J., and Dohlman, H. G. (2008) *Curr. Biol.* **18,** 211–215
31. Dohlman, H. G., Goldsmith, P., Spiegel, A. M., and Thorner, J. (1993) *Proc. Natl. Acad. Sci. U.S.A.* **90,** 9688–9692
32. Rasband, W. S. (1997–2009) *U.S. National Institutes of Health, Bethesda, Maryland*
33. Asano, S., Park, J. E., Yu, L. R., Zhou, M., Sakchaisri, K., Park, C. J., Kang, Y. H., Thorner, J., Veenstra, T. D., and Lee, K. S. (2006) *J. Biol. Chem.* **281,** 27090–27098
34. Hoffman, G. A., Garrison, T. R., and Dohlman, H. G. (2002) *Methods Enzymol.* **344,** 617–631
35. Studier, F. W. (2005) *Protein Expr. Purif.* **41,** 207–234
36. Wedegaertner, P. B., Wilson, P. T., and Bourne, H. R. (1995) *J. Biol. Chem.* **270,** 503–506
37. Stone, D. E., Cole, G. M., de Barros Lopes, M., Goebl, M., and Reed, S. I. (1991) *Genes Dev.* **5,** 1969–1981
38. Li, X., Gerber, S. A., Rudner, A. D., Beausoleil, S. A., Haas, W., Villén, J., Elias, J. E., and Gygi, S. P. (2007) *J. Proteome Res.* **6,** 1190–1197
39. Sreenivasan, A., and Kellogg, D. (1999) *Mol. Cell. Biol.* **19,** 7983–7994
40. Szkotnicki, L., Crutchley, J. M., Zyla, T. R., Bardes, E. S., and Lew, D. J. (2008) *Mol. Biol. Cell* **19,** 4675–4686
41. Crutchley, J., King, K. M., Keaton, M. A., Szkotnicki, L., Orlando, D. A., Zyla, T. R., Bardes, E. S., and Lew, D. J. (2009) *Mol. Biol. Cell* **20,** 1926–1936
42. Bouquin, N., Barral, Y., Courbeyrette, R., Blondel, M., Snyder, M., and Mann, C. (2000) *J. Cell Sci.* **113,** 1435–1445
43. Koehler, C. M., and Myers, A. M. (1997) *FEBS Lett.* **408,** 109–114
44. Palecek, S. P., Parikh, A. S., and Kron, S. J. (2000) *Genetics* **156,** 1005–1023
45. Manderson, E. N., Malleshaiah, M., and Michnick, S. W. (2008) *PLoS ONE* **3,** e1500
46. Weinert, T. A., Kiser, G. L., and Hartwell, L. H. (1994) *Genes Dev.* **8,** 652–665
47. Jacobs, C. W., Adams, A. E., Szaniszlo, P. J., and Pringle, J. R. (1988) *J. Cell Biol.* **107,** 1409–1426
48. Deshaies, R. J. (1997) *Curr. Opin. Genet. Dev.* **7,** 7–16
49. Liang, C., Weinreich, M., and Stillman, B. (1995) *Cell* **81,** 667–676
50. Liang, C., and Stillman, B. (1997) *Genes Dev.* **11,** 3375–3386
51. Finley, D., Tanaka, K., Mann, C., Feldmann, H., Hochstrasser, M., Vierstra, R., Johnston, S., Hampton, R., Haber, J., McCusker, J., Silver, P., Frontali, L., Thorsness, P., Varshavsky, A., Byers, B., Madura, K., Reed, S. I., Wolf, D., Jentsch, S., Sommer, T., Baumeister, W., Goldberg, A., Fried, V., Rubin, D. M., and Toh-e, A. (1998) *Trends Biochem. Sci* **23,** 244–245
52. Ellison, M. J., and Hochstrasser, M. (1991) *J. Biol. Chem.* **266,** 21150–21157
53. Hochstrasser, M., Ellison, M. J., Chau, V., and Varshavsky, A. (1991) *Proc. Natl. Acad. Sci. U.S.A.* **88,** 4606–4610
54. Skowyra, D., Craig, K. L., Tyers, M., Elledge, S. J., and Harper, J. W. (1997) *Cell* **91,** 209–219
55. Neiman, A. M., Chang, F., Komachi, K., and Herskowitz, I. (1990) *Cell Regul.* **1,** 391–401
56. Caydasi, A. K., Kurtulmus, B., Orrico, M. I., Hofmann, A., Ibrahim, B., and Pereira, G. (2010) *J. Cell Biol.* **190,** 975–989
57. Hedbacker, K., and Carlson, M. (2008) *Front. Biosci.* **13,** 2408–2420
58. Suchkov, D. V., DeFlorio, R., Draper, E., Ismael, A., Sukumar, M., Arkowitz, R., and Stone, D. E. (2010) *Mol. Biol. Cell* **21,** 1737–1752

Cell Cycle-dependent Phosphorylation and Ubiquitination of a G Protein α Subunit

Matthew P. Torres, Sarah T. Clement, Steven D. Cappell and Henrik G. Dohlman

J. Biol. Chem. 2011, 286:20208-20216.
doi: 10.1074/jbc.M111.239343 originally published online April 26, 2011
